DIFFERENT APPROACHES TO DEPICT FATIGUE OF BITUMINOUS MATERIALS

I. Artamendi and H. Khalid
Dept. of Civil Engineering, University of Liverpool
Brownlow Street, L69 3GQ, Liverpool, UK
ignacio@liv.ac.uk and khalid@liv.ac.uk

Abstract

This study investigates the fatigue characteristics of typical bituminous materials used in road applications. Fatigue testing was performed in a four-point bending beam test apparatus under controlled strain and stress conditions. Fatigue life was defined using the classical approach as the number of cycles, N_f, to 50% reduction in the initial stiffness modulus. It has also been defined in terms of macro-crack initiation, N_1. A different approach, based on the linear reduction in stiffness during a particular stage of a fatigue test, was introduced to define a damage parameter and the evolution of this damage parameter with number of cycles was used to characterise fatigue life. Furthermore, refinements to the linear damage model were introduced to take into account the difference in the evolution of dissipated energy between controlled strain and stress testing modes. These modifications have enabled the identification of a unique fatigue damage rate for both controlled strain and stress test modes.

1. Introduction

Fatigue cracking is one of the major load-related distresses experienced in asphalt pavements and occurs when a bituminous layer is subjected to repeated loading under the passing traffic. In the laboratory, fatigue life is typically assessed by repeated-load bending tests. Three configurations are mainly employed, two-point bending or trapezoidal beam test, and three or four-point bending tests.

Fatigue tests are carried out in two modes, controlled strain and controlled stress. In controlled strain mode, the strain is kept constant by decreasing the stress during the test whereas in controlled stress the stress is maintained constant which increases the strain during the test. In general, controlled stress testing has been related to relatively thick pavement construction where high stiffness is the fundamental parameter that underpins fatigue life. Controlled strain testing, on the other hand, has been associated with thin conventional flexible pavements where the elastic recovery properties of the material have a fundamental effect on its fatigue life.

Different approaches have been used to define the fatigue life of bituminous materials. Failure in controlled strain has been widely defined as 50% reduction in the initial stiffness modulus (Tayebali *et al.* [1]). For controlled stress testing, on the other hand, fatigue failure has been traditionally considered to occur when the modulus is at 10% of its original value (van Dijk and Visser [2]). These definitions, however, are considered arbitrary and do not represent the internal state of the material.

Hopman *et al.* [3] and Pronk [4] introduced an energy ratio, R_n, based on the dissipated energy concept and defined failure as the number of cycles, N_1, where cracks are considered to form. In controlled strain mode, when R_n is plotted against the number of cycles, N_1 is

defined as the point where the slope of R_n against N deviates from a straight line. In controlled stress mode, on the other hand, N_1 corresponds to the peak value of R_n. For controlled strain and stress modes, N_1 represents the material in the same state of damage corresponding to macro-crack initiation (Rowe [5]). It is, however, more difficult and subjective to accurately define the N_1 point for strain mode than for stress mode.

Di Benedetto *et al*. [6, 7] proposed a different approach to characterize fatigue. They identified the existence of a stage during a fatigue test, which accounted for most of the fatigue life, where the reduction in the stiffness with number of load applications was approximately linear. Based on this, a damage parameter (D) was introduced and the change in this parameter with number of cycles has been used to depict damage due to fatigue. Furthermore, the model proposed by Di Benedetto *et al*. introduced an energy term to counteract the variability due to dissipated energy effects in the two modes of loading.

The objective of this paper is to investigate the fatigue characteristics of two typical bituminous materials, namely Dense Bitumen Macadam (DBM) and Stone Mastic Asphalt (SMA), used in road applications in the UK. The energy ratio and linear damage evolution approaches used to depict fatigue life have been applied and compared with the arbitrary approach.

2. Fatigue test procedures

Fatigue testing was performed in a four-point bending (4PB) test apparatus shown schematically in Fig. 1. The test equipment consisted of a servo-hydraulic actuator connected to a 2.5 kN load cell mounted above the fatigue frame. The load was applied through the actuator that was connected to the fatigue frame by means of a steel shaft. Once inserted the specimen was clamped in position at the four points of the fatigue frame by means of torque motors located underneath the four supports.

The vertical deflection at the centre of the beam was measured using a Linear Variable Differential Transducer (LVDT) situated at the bottom of the beam. The transducer was pushed into contact with the specimen by means of a pneumatically controlled trigger mechanism prior to start of the test. The vertical deflection and the applied load were used to calculate the strains and stresses. Furthermore, phase angle, dissipated energy and cumulative dissipated energy were also computed during the test.

Beam specimens of 300x50x50mm^3 were cut from 300x300mm^2 slabs manufactured in the laboratory and used for fatigue testing. All tests were conducted at a temperature of 10 ^{0}C and 10 Hz frequency, under sinusoidal loading with no rest periods. Testing was carried out under controlled strain and stress conditions. For controlled strain testing, strain amplitude levels selected varied between 125 and 200 μm/m. For controlled stress testing, stress amplitude levels selected varied between 1.25 and 2 MPa.

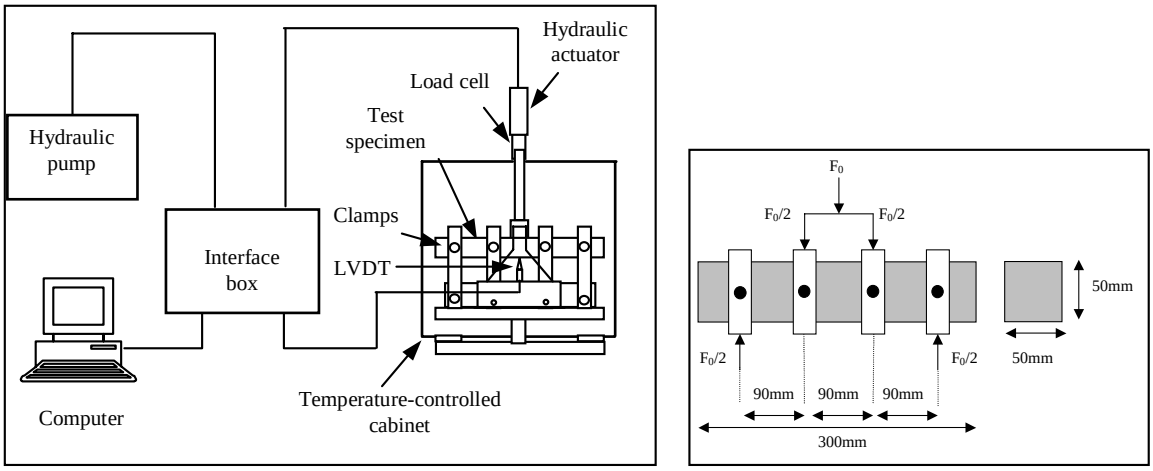

FIGURE 1. 4PB test apparatus and test configuration

3. Characterisation of fatigue life

3.1 Definition of failure based on stiffness reduction

Fatigue failure has been arbitrarily defined as the number of cycles, N_f, at which the initial stiffness is reduced by 50%, for both controlled strain and stress test modes. Typical fatigue data from 4PB tests for controlled strain and stress tests are presented in Fig. 2. This data corresponds to two DBM beam specimens under similar initial strain conditions of 153 and 152.2 μm/m. It can be seen that, under these conditions, failure in controlled stress mode occurred considerably earlier than in controlled strain mode.

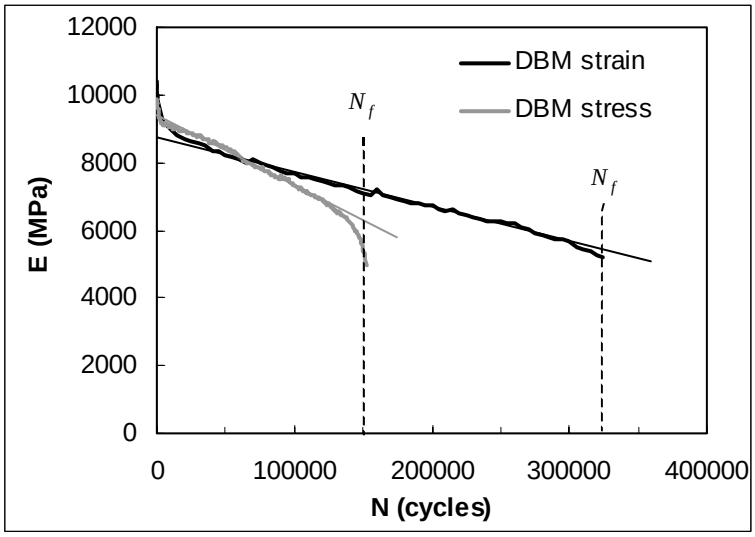

FIGURE 2. Definition of failure N_f in controlled strain and stress test mode

Fatigue test data in controlled strain and stress mode has been used to derive a relationship between the initial strain and fatigue life, N_f, as shown in Fig. 3. It can be observed that, firstly, fatigue life for the SMA material was longer than that for the DBM material, independent of the test mode and, secondly, fatigue lives from controlled stress tests were shorter than those from controlled strain tests for both materials. Longer lives for the SMA material are attributed to volumetric composition and type of bituminous binder. Shorter lives in controlled stress mode are due to higher rate of crack propagation in this mode as it is a

function of the stress magnitude at the crack tip. In controlled strain mode, on the other hand, there is a gradual reduction in the applied stress as the material weakens.

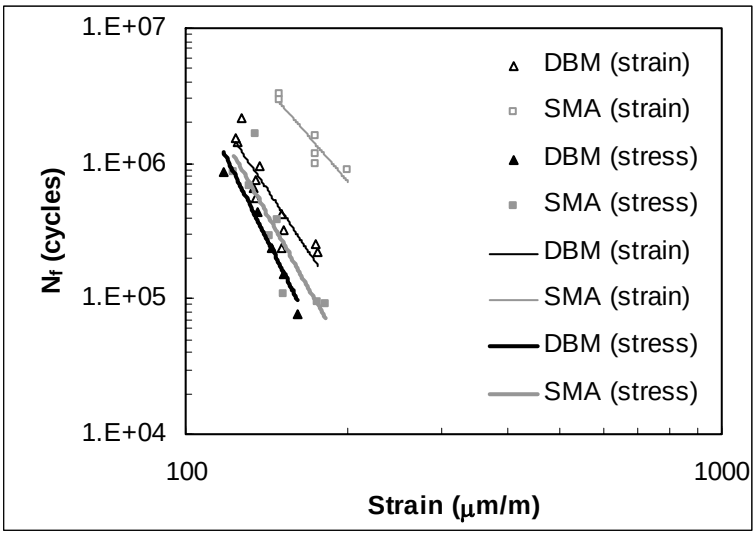

FIGURE 3. Relationship between fatigue life N_f and initial strain

3.2 Definition of failure based on Energy Ratio

An Energy Ratio, R_n, has been used to define the number of cycles, N_1, where macro-cracks are considered to initiate. The energy ratio is defined as the quotient between the cumulative dissipated energy up to the n-cycle and the dissipated energy at the n-cycle. Thus,

$$R_n = \frac{\pi \sum_{i=0}^{n} \sigma_i \varepsilon_i \sin \phi_i}{\pi \sigma_n \varepsilon_n \sin \phi_n} \tag{1}$$

where σ, ε and ϕ are the stress, strain and phase angle respectively.

Fig. 4 shows the evolution of R_n with number of cycles for the two specimens presented in Fig. 2. It can be seen that for controlled strain mode, when R_n is plotted against the number of load cycles there is a change in behaviour at N_1 represented by the change of the slope at this point. The accurate determination of N_1 is, however, somewhat subjective. In controlled stress test mode, on the other hand, N_1 corresponds to the peak value when R_n is plotted against the number of load cycles. Furthermore, under similar initial strain conditions, N_1 is lower for controlled stress than for controlled strain mode, as shown in Fig. 4. Also, crack initiation, indicated by N_1, occurred before the attainment of 50% reduction in stiffness, i.e. at N_f.

The relationship between N_1 and the initial strain for controlled strain and stress tests is presented in Fig. 5. It can be seen that, again, the SMA material had longer fatigue life than the DBM for both test modes, and similarly fatigue life, N_1, for controlled stress mode was shorter than for controlled strain. Furthermore, the scatter observed in Fig. 5 (and Fig. 3) is representative of typical scatter inherent in fatigue test results.

Although fatigue tests gave similar relationships for N_1 and N_f, the N_1 failure criterion allows a comparison of materials at equal states of damage, corresponding to macro-crack initiation, and avoids arbitrary definition of failure.

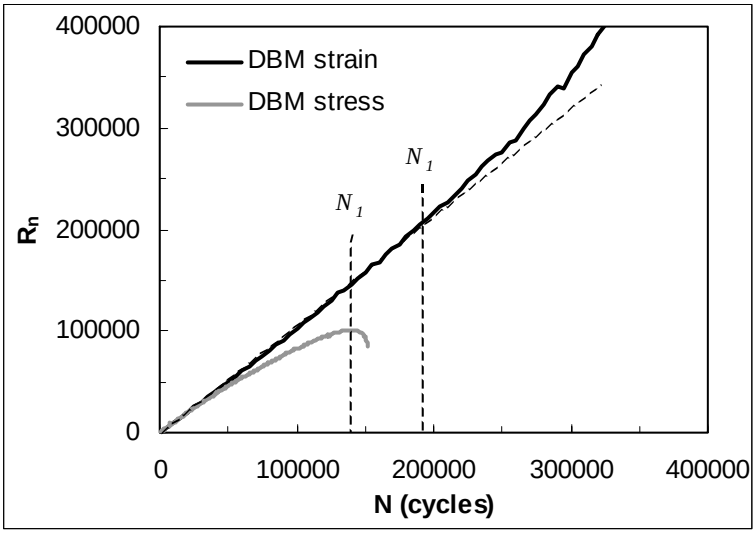

FIGURE 4. Definition of failure N_1 in controlled strain and stress test modes

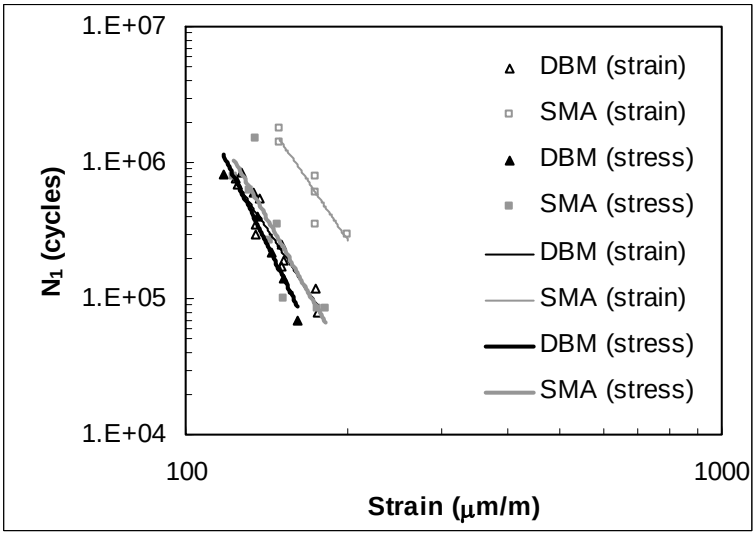

FIGURE 5. Relationship between fatigue life N_1 and initial strain

3.3 Definition of fatigue damage

Fatigue data from 4PB tests has shown the existence of a stage during the test characterised by an approximately linear reduction in the stiffness modulus, E, with number of cycles, as shown in Fig. 2. Based on this linear reduction in the stiffness a damage parameter, D, can be introduced. Thus,

$$D(N) = \frac{E_{00} - E(N)}{E_{00}} \tag{2}$$

The rate of damage can be calculated by differentiating Equation 2.

$$\frac{dD}{dN} = -\frac{1}{E_{00}}\frac{dE}{dN} = -a_T \tag{3}$$

where E_{00} and dE/dN are the intercept and the slope of the fitted line for the stiffness data, as shown in Fig. 2.

The relationship between *dD/dN* and the initial strain for both test modes was approximated by a power law, which gave regression coefficients (R^2) of about 0.8 for both tested materials. These relationships are presented in Fig. 6. It can be observed that, as expected, for the same initial strain, the rate of damage for controlled stress tests is higher than that for controlled strain tests. It can also be seen that the rate of damage for the DBM material is higher than that for the SMA material, independent of test mode. These observations are attributed to the same reasons given in section 3.1.

Differences between the rate of damage for controlled strain and stress tests have been attributed to dissipated energy effects occurring in both test modes [6, 7]. During controlled strain fatigue testing the dissipated energy decreases with *N* and increases during controlled stress tests, as shown in Fig. 7. Furthermore, under similar initial strain conditions, the rate of change (slope) in dissipated energy with load cycles is faster for controlled stress than for controlled strain mode (see Fig. 7).

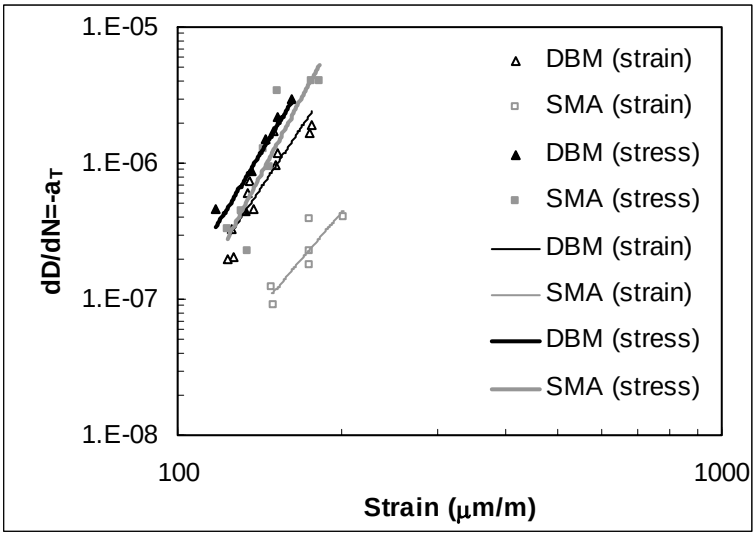

FIGURE 6. Relationship between rate of damage *dD/dN* and initial strain

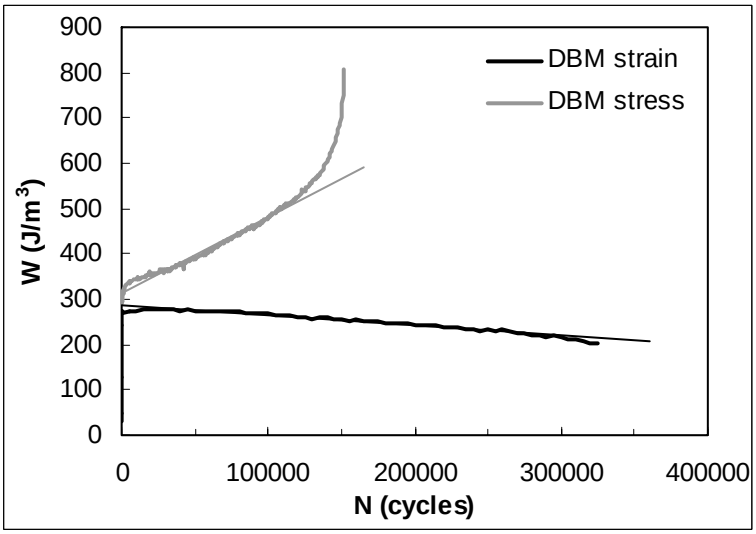

FIGURE 7. Evolution of dissipated energy in controlled strain and stress test modes

As a result of the energy differences, the proposed relationship to determine the corrected rate of damage, dD^*/dN, can be expressed as follows [7].

$$\frac{dD^*}{dN} = -a_T - C\left(\frac{E_0 - E_{00}}{E_{00}}\right)a_W \tag{4}$$

where E_0 is the initial stiffness, C is a material's constant and a_W is defined as follows.

$$a_W = \frac{1}{W_{00}}\frac{dW}{dN} \tag{5}$$

where W_{00} and dW/dN are the intercept and the slope of the fitted line for the dissipated energy data, as shown in Fig. 7.

Fig. 8 shows a power law relationship between a_W (absolute values) and the initial strain for both controlled strain and stress tests, which gave R^2 values between 0.7 and 0.9. It can be seen that a_W values for controlled stress tests are higher than for controlled strain ones, as explained earlier (see Fig. 7). Moreover, a_W values for the DBM material are higher than those for the SMA material, emphasising DBM's inferior resistance to fatigue cracking.

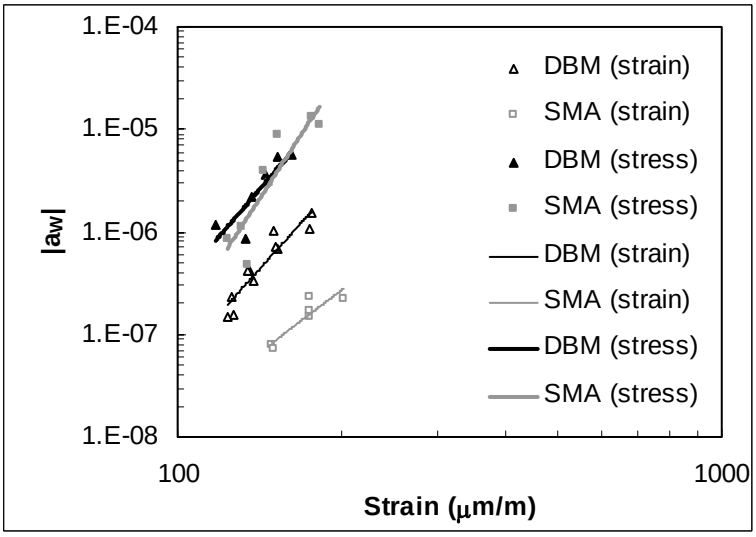

FIGURE 8. Relationship between the parameter a_W and the initial strain

Finally, a power law relationship was found between the corrected rate of damage, dD^*/dN, calculated using Equation 4, and the initial strain for both test modes. The values of the constant C were determined by using an iterative method which aimed at maximising the R^2 value for this relationship. The values of the constant C determined in this way were 1.95 and 2.05 for the DBM and SMA materials respectively, which gave R^2 values of 0.8 for both materials.

The relationship between dD^*/dN and initial strain for controlled strain and stress tests for the two materials investigated is presented in Fig. 9. The figure shows a unique damage relationship for each material, irrespective of test mode.

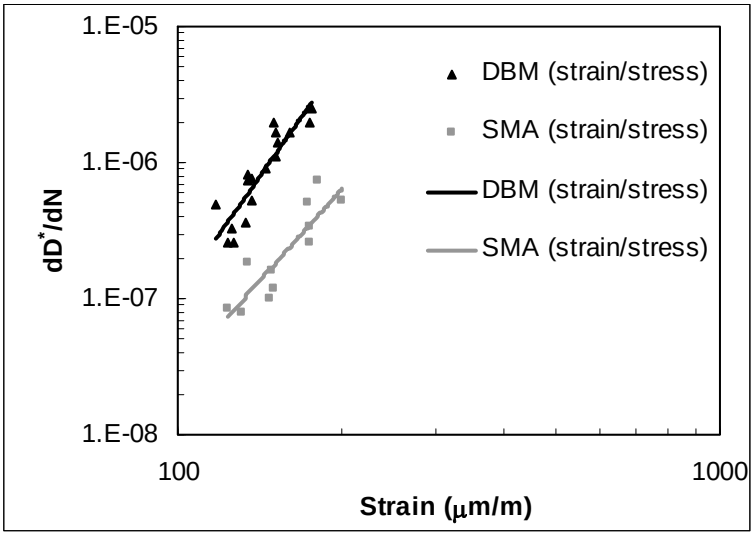

FIGURE 9. Relationship between the corrected damage rate and the initial strain

4. Conclussions

Fatigue results presented in terms of N_f and N_1 have demonstrated that fatigue lives could be presented in either format, although N_1 is more preferable as it relates to an internal state of the material. The interpretation of N_1 from either test mode, however, is prone to some subjectivity.

The linear damage model proposed by Di Benedetto has ranked the SMA and DBM materials in the same manner as the more classical approach. The corrected rate of damage approach is useful in depicting the material's fatigue behaviour in that it identifies a unique damage rate independent of the test mode.

References

1. Tayebali, A.A., Rowe, G.M. and Sousa, J.B., *J. Assoc. Asphalt Paving Technologists*, vol. **61**, 333-360, 1992.
2. van Dijk, W and Visser, W., *J. Assoc. Asphalt Paving Technologists*, vol. **46**, 1-40, 1977.
3. Hopman, P.C., Kunst, P.A. and Pronk, A.C. In *Proceedings of the Forth Eurobitume Symposium*, Madrid, 1989, 557-561.
4. Pronk, A.C., In *Proceedings of the Eighth International Conference on Asphalt Pavements*, Seattle, 1997, 987-994.
5. Rowe, G.M., *J. Assoc. Asphalt Paving Technologists*, vol. **62**, 344-384, 1993.
6. Di Benedetto, H., Ashayer Soltani, M.A. and Chaverot, P., *J. Assoc. Asphalt Paving Technologists*, vol. **65**, 142-158, 1996.
7. Di Benedetto, H., de La Roche, C., Baaj, H., Pronk, A. and Lundstron, R., In *Proceedings of the Sixth International RILEM Symposium*, Zurich, 2003, 15-38.